Journal of Cranio-Maxillo-Facial Surgery 47 (2019) 1162–1169

Contents lists available at ScienceDirect

Journal of Cranio-Maxillo-Facial Surgery

journal homepage: www.jcmfs.com

Medication-related osteonecrosis of the jaw in a minipig model: Parameters for developing a macroscopic, radiological, and microscopic grading scheme

B. Nowicki [a], D. Nehrbass [a], D. Arens [a], V.A. Stadelmann [a], S. Zeiter [a], S. Otto [b], P. Kircher [c], M.J. Stoddart [a, d, *]

[a] AO Research Institute Davos, Davos Platz, Switzerland
[b] Department of Oral and Maxillofacial Surgery, University of Munich, Munich, Germany
[c] Department of Veterinary Radiology, University of Zurich, Zurich, Switzerland
[d] Medical Faculty, Albert Ludwigs University of Freiburg, Freiburg, Germany

ARTICLE INFO

Article history:
Paper received 31 October 2018
Accepted 1 March 2019
Available online 18 March 2019

Keywords:
Bisphosphonate
Osteonecrosis
BRONJ
Minipig
Histopathology
Computed tomography

ABSTRACT

Objectives: To devise a macroscopic, radiological, and histological scale for assessing pathological changes associated with medication-related osteonecrosis of the jaw in a minipig model.
Materials and methods: Medication-related osteonecrosis of the jaw was induced in Göttingen minipigs by weekly intravenous administration of bisphosphonate (zoledronic acid) combined with a tooth extraction procedure. Controls either did not receive zoledronic acid or did not undergo tooth extraction. After 20 weeks, minipigs were euthanized and underwent computed tomography and micro-computed tomography scanning. The mandible underwent additional histological examination.
Results: The most consistent macroscopic findings in animals that had developed bisphosphonate-related osteonecrosis of the jaw (BRONJ) were necrotic, denuded bone, and formation of fistula and pus. Under radiological examination, impaired extraction socket healing, decrease in attenuation of bone beneath the extraction site, and periosteal reaction were observed. Under histological examination, demineralization of the extracellular bone matrix, denuding of bone, and osteonecrosis were recorded.
Conclusion: These parameters were used to develop a scoring system for grading BRONJ.

1. Introduction

Bisphosphonates (BPs) are anti-resorptive drugs widely used to treat osteoporosis, Paget's disease, malignant hypercalcemia, or resorptive skeletal alterations associated with metastatic malignancies (Sambrook and Cooper, 2006; Hatoum et al., 2008). While being very effective in restoring bone density (Major et al., 2001), a rare but severe clinical condition called bisphosphonate-related osteonecrosis of the jaw (BRONJ), also known as medication-related osteonecrosis of the jaw (MRONJ), is observed during treatment with these otherwise well tolerated drugs (Wang et al., 2003; Marx, 2003; Migliorati, 2003).

BRONJ was first observed in 2003 (Wang et al., 2003; Marx, 2003; Migliorati, 2003) and is currently only described by anamnestic and clinical features. The American Society for Bone and Mineral Research definition (Khosla et al., 2007) adopted by the American Association of Oral and Maxillofacial Surgeons (Ruggiero et al., 2009) defines it as involving: (a) the presence of exposed bone in the oral cavity for a period that exceeds 8 weeks; (b) a positive BP drug history; and (c) no prior irradiation to the head and neck region. This definition suggests BP treatment as a risk factor for BRONJ, but to date the importance of BP and its underlying pathogenesis is still under discussion (Novince et al., 2009; Kumar and Sinha, 2013; Cheung and Seeman, 2010). For this reason, a large animal tooth extraction model using Göttingen minipigs (Pautke et al., 2012; Otto et al., 2017) was established to largely represent the human situation.

Since the full extent of pathological changes related to MRONJ is not always detectable in clinical examination, computed

* Corresponding author. AO Research Institute Davos, Clavadelerstrasse 8, 7270, Davos Platz, Switzerland.
E-mail address: Martin.stoddart@aofoundation.org (M.J. Stoddart).

https://doi.org/10.1016/j.jcms.2019.03.002
1010-5182/

tomography (CT) is increasingly playing a role in screening, detecting, staging, and monitoring the patients (Torres et al., 2012; Hutchinson et al., 2010; Arce et al., 2009; Hamada et al., 2014). As it is critically important to know the differences and similarities between animal models and clinical patients, careful examination of radiological findings in minipigs, and their comparison with findings from patients, is warranted.

Histopathology is crucial for understanding pathological processes accompanying diseases. To better understand MRONJ, it is important to carry out careful histopathological examinations of animal models, and to correlate these with clinical findings to provide a clinically applicable assessment.

The aim of this study was to establish a scale to allow reproducible assessment of clinical, radiological, and histopathological findings in a minipig tooth extraction model, and to correlate these with the clinical manifestation of MRONJ in humans. The animal outcomes were previously published (Otto et al., 2017). This paper focuses on the development of a scoring system that could then be used to unify reporting in future BRONJ studies.

2. Materials and methods

In order to develop this scoring system, a number of radiological and histological parameters to be investigated across the different groups were defined by the authors. These parameters were chosen because they were relatively easy to establish. Based on the results, those parameters demonstrating a clear difference between animals that did develop MRONJ and those that did not were included in the scoring system.

2.1. Methods of obtaining data

All procedures during the study were carried out in an AAALAC-accredited facility, in accordance with the Swiss laws governing animal welfare, and were approved by the cantonal and federal Animal Welfare Commissions of the official veterinary authorities (Authorization Number 03_2012). Acclimatization, housing, and feeding were conducted as previously published (reference 13).

Twelve female Göttingen minipigs (18–21 months; 39.1 ± 4.4 kg) were randomly assigned to one of three groups. Group 1 ($n = 3$) had only bisphosphonate administration; group 2 ($n = 6$), tooth extraction and bisphosphonate administration; and group 3 ($n = 3$), only tooth extraction. Zoledronic acid (ZOL) was administered intravenously to the bisphosphonate groups (0.05 mg/kg, once a week) through the whole duration of the study (20 weeks), under sedation (ketamine (15 mg/kg), midazolam (0.5 mg/kg), and azaperon (2 mg/kg) — all intramuscular).

After 11 weeks of ZOL injections (for group 2), tooth extraction was performed. All animals were fasted 24 h prior to surgery and premedicated, as described above. Induction was achieved with an intravenous injection of propofol (3–5 mg/kg). Animals were than intubated (armored endotracheal tube) and isoflurane (Et(Iso) 1–1.5%) in 0.6–1 l/min of oxygen and air was administered to maintain anesthesia.

For analgesic purposes, carprofen (4 mg/kg intravenously) was administered before the beginning of extraction. A local nerve block of mandibular and maxillary nerve branches at the extraction location was performed using lidocaine 2% and bupivacain 0.5%, with 1:200,000 adrenaline solution.

Unilateral extraction of four premolar (PM) teeth was performed. Using a set of different-sized elevators, the marginal paradont of each tooth was freed and the tooth was mobilized until movement. PM2 (mandible and maxilla) and PM4 (mandible only) were split into two parts in the transverse plane using a high-speed instrument. PM4 (maxilla only) was split along the fissures into three parts, in a star-shaped pattern (one palatinal root and two buccal roots). The fragments were carefully mobilized and extracted. Analgesia was maintained using buprenorphine (0.02 mg/kg intramuscularly) for the first 24h postoperatively, fentanyl patches (50 μg/h) for the first 3 days postoperatively, and carprofen (4 mg/kg intramuscularly) 5 days postoperatively. The extraction side was evaluated on a weekly basis by means of visual inspection, and scored according to a BRONJ scoring scale described by Ruggiero et al. (2009). After 20 weeks from the beginning of the study, all animals were euthanized with an overdose of pentobarbital, injected via the auricular vein.

Clinical CT scans were acquired immediately after euthanasia. The scanner (SOMATOM Emotion 6, Siemens, Erlangen, Germany) was operated with a tube voltage of 130 kVp and tube current of 125 mA; the acquired images had an in-plane resolution of 0.5 mm and a slice thickness of 0.63 mm, and were reconstructed with a sharp convolution kernel (H70s).

Animals were necropsied and mandibles (cut in half — left/right) were scanned again using a microCT scanner (XtremeCT, Scanco Medical AG) operated at 60 kV and 900 μA, with 750 projections and 200 ms acquisition time in a 126 mm field of view. The slices were reconstructed across an image matrix size of 1536 × 1536 voxels, with a nominal voxel size of 82 μm.

For histological analyses the left-side mandible with PM4 extraction and the right-side mandible without PM4 extraction were fixed in 70% methanol, trimmed, and cut along the sagittal plane with a diamond-blade saw (Exact, Norderstedt, Germany). The lingual half of the tissue, was transferred to xylene, embedded in methylmethacrylate (MMA), and further cut in consecutive sections with a thickness of approximately 300–500 μm. The slides were then glued onto opaque plexiglas holders, ground down to approximately 175–250 μm thickness, and stained with Giemsa-Eosin (Fig. 1b). Before mounting and staining, contact radiographies of the sections were taken using high-resolution technical films (D4 Structurix DW ETE, Agfa) and a cabinet X-ray system (Model No. 43855A, Faxitron X-Ray Corporation), applying the following settings: 20 kV for 40 sec, no filter, 56 cm source-to-image distance.

2.2. Methods of evaluation

The criteria used for clinical scoring throughout the study are listed in Table 1.

Clinical observations were recorded weekly, under sedation, by means of visual inspection of the oral cavity.

All CT scans were assessed using a commercially available computer program (Osirix, Switzerland). Hounsfield units (HU), bone mineral density (BMD), and volumetric measurements were computed using the software's 'region of interest' (ROI) tools.

A semi-quantitative and quantitative grading scheme was developed to assess radiological and histological changes associated with MRONJ.

The following parameters were evaluated from CT scans of mandibles: periosteal reaction; soft tissue swelling; empyema; healing of extraction socket; mean attenuation of trabecular bone area under PM4, M1, and M2; periodontal ligament space of PM4 and M1; total bone volume; and bone mineral density (BMD) of mandible between PM3 and M1, and between PM2 and M3 (Table 2).

Semi-quantitative light microscopic analysis, using a grading scheme (grades 0–5), was performed on the left-sided tooth extraction sites of the mandibular PM4.

Among others, the following parameters were analyzed and graded: inflammation of gingiva, periodontium, or of the pulp of adjacent teeth (gingivitis, periodontitis, pulpitis); inflammation of

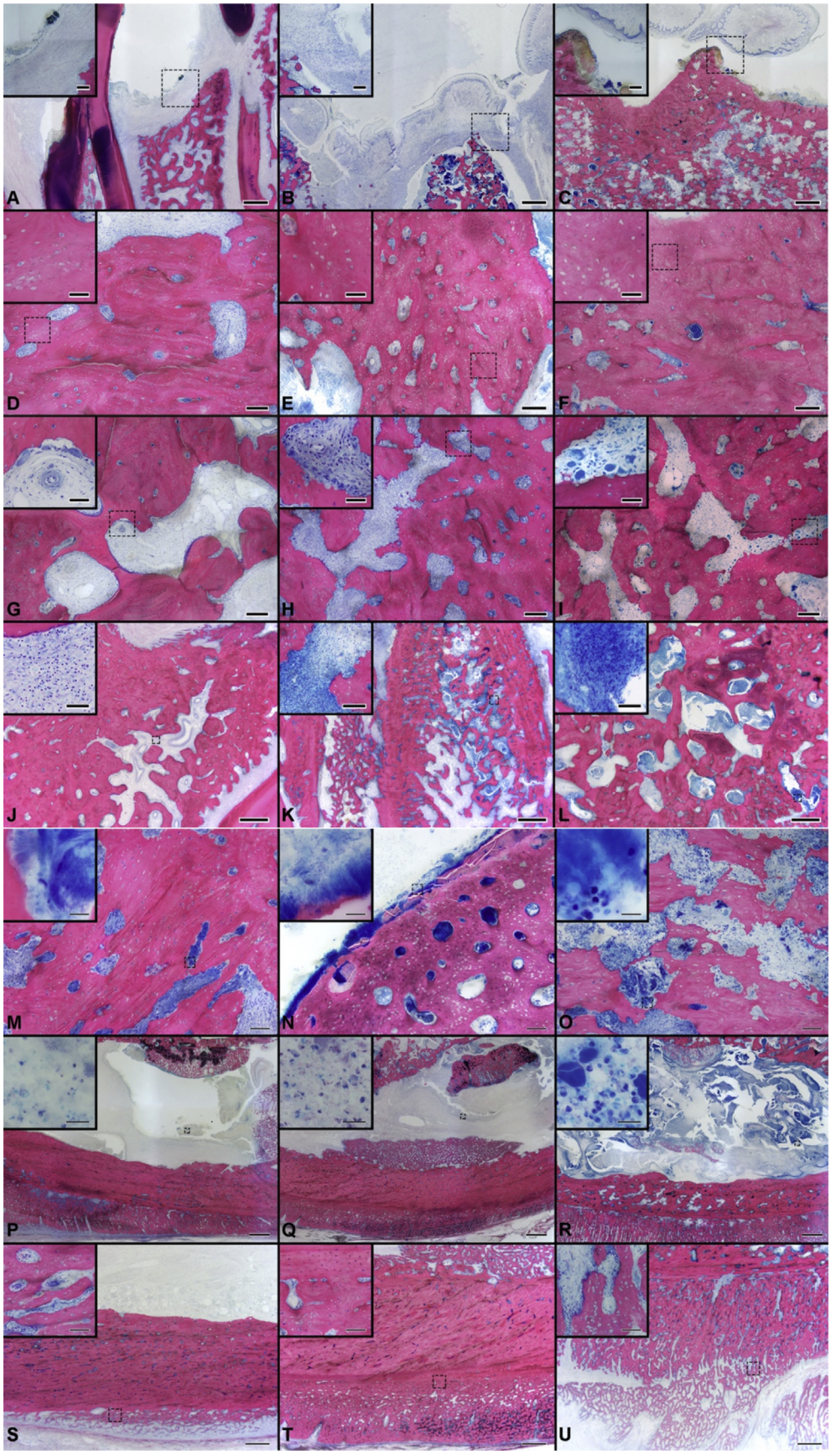

Fig. 1. Ranking of selected histopathological tissue changes according to a five-point scale (grades 0–5). Methanol-fixed, undecalcified, MMA-embedded, Giemsa-eosin-stained mandibular tissue sections from minipigs treated with zoledronate (except samples A, D, G, J, which are of untreated animals and show typical background changes). The left-hand

Table 1
MRONJ stage descriptions (Ruggiero et al., 2014).

At risk category	No apparent necrotic bone in patients who have been treated with either oral or IV bisphosphonates
Stage 0	No clinical evidence of necrotic bone, but non-specific clinical findings, radiographic changes, and symptoms
Stage 1	Exposed and necrotic bone, or fistulae that extend to bone, in patients who are asymptomatic and have no evidence of infection
Stage 2	Exposed and necrotic bone, or fistulae that extend to bone, associated with infection, as evidenced by pain and erythema in the region of the exposed bone with or without purulent drainage
Stage 3	Exposed and necrotic bone or a fistula that extends to bone in patients with pain, infection, and one or more of the following: exposed and necrotic bone extending beyond the region of alveolar bone (i.e. inferior border and ramus in the mandible, maxillary sinus, and zygoma in the maxilla) resulting in pathologic fracture; extraoral fistula; oral antral/oral nasal communication; or osteolysis extending to the inferior border of the mandible of the sinus floor

the bone and bone marrow of the jaw (osteomyelitis); pus accumulation in the canalis mandibularis/sinus maxillaris (empyema); presence of Giemsa-positive bacterial colonies (infection); presence of osteoblasts on the trabecular surface (bone formation); presence of Howship lacunae on the trabecular surface, with or without presence of osteoclasts (osteolysis); foci of $n > 5$ empty osteocytic lacunae (osteonecrosis); and incomplete gingival epithelial wound closure of the extraction site (gingival ulceration without/with exposed denuded bone (characterized by demineralization of bone matrix) (Table 3).

3. Results

All animals that received zoledronic acid developed symptoms associated with MRONJ.

3.1. Macroscopic changes

In animals that developed MRONJ, a gradual increase in disease stage was observed and clinical macroscopic findings, including gingivitis, exposed necrotic bone, infection, purulent discharge, fistula formation, abscess formation, and soft tissue swelling, were recorded. No such clinical changes were observed in the control group.

Table 2
Radiological grading scheme for semi-quantitative and quantitative scoring: grade 0 = absent, grade 1 = minimal, grade 2 = slight, grade 3 = moderate, grade 4 = marked/severe, grade 5 = massive.

Radiological change	Grade
Periosteal reaction	0–5
Soft tissue swelling	0–5
Empyema	Presence/absence
Healing of extraction socket	Presence/absence
Mean attenuation of area of trabecular bone directly under M2	HU value
Mean attenuation of area of trabecular bone directly under M1	HU value
Mean attenuation of area of trabecular bone directly under PM4	HU value
Periodontal ligament space, M1	mm value
Periodontal ligament space, PM4	mm value
Bone volume of mandible in area between PM3 and M1	mm^3 value
Bone mineral density of mandible in area between PM3 and M1	(CaHa)g/cm^3 value
Bone volume of mandible in area between PM2 and M3	mm^3 value
Bone mineral density of mandible in area between PM2 and M3	(CaHa)g/cm^3 value

3.2. Radiological changes

3.2.1. Clinical CT

Left and right mandible CT scans were evaluated and a variety of pathological changes were observed. One of the most striking was a periosteal reaction: minipigs that developed MRONJ showed marked to massive periosteal and endosteal reaction at the corpus mandibulae. This was located not only near the extraction side, but also on the other side of the jaw, and was also observed in animals that were exposed to bisphosphonate but did not undergo tooth extraction. Soft tissue swelling visible under these scanning conditions was strongly associated with periosteal reaction/calcification, and both phenomena were observed at a similar rate.

3.2.2. Empyema (pus in the canalis mandibularis) was present in most of the animals that developed MRONJ

Healing of the extraction socket was markedly impaired in all animals that received zoledronic acid, but in none of the animals from the control group (tooth extraction only). Mean attenuation values for trabecular bone were measured at different locations (PM4, M1, M2) near the extraction site. Some of the animals

column shows changes of low severity (grade 1), the center column those of moderate severity (grade 3), and the right-hand column those of high severity, characteristically observed in MRONJ (grade 4). Panels,**A–C, gingival ulceration** (bar 1 cm; inset bar 200 μm). **Panel A**: (grade 1): note the small, focused disruption of the mucosal basal membrane in direct proximity to food material (see inset) and accompanied with moderate inflammatory cell infiltration of the submucosa but not of the underlying bone stock. **Panel B**: (grade 3): Note the multifocal mucosal disruption, accompanied with severe inflammatory cell infiltration of the submucosa and of the underlying bone stock. **Panel C**: (grade 4): note the severe mucosal discontinuity leading to orally denuded bone, demineralization of extracellular bone matrix, colonization with bacterial oral flora (inset), and marked inflammatory cell infiltration of the bone stock. **Panels D–F, osteonecrosis**: (bar 200 μm; inset bar 50 μm). **Panel D**: (grade 1): note the single focus of >5 empty osteocytic lacunae (inset); the rest of the bone stock visible is vital, with living osteocytes remaining in the lacunae. **Panel E**: (grade 3): a large percentage of the lacunae of the bone area shown are empty (inset). **Panel F**: (grade 4): in the area shown, all osteocytic lacunae are empty; note the irregular shape of the empty lacunae (inset). **Panels G–I, osteolysis**: (bar 200 μm; inset bar 50 μm). **Panel G**: (grade 1): note the focused presence of a few osteoclasts forming semilunar-shaped Howship lacunae (inset); the vast majority of the bone surface is occupied by osteoblasts. **Panel H**: (grade 3): the bone surface is irregular and largely occupied by osteoclasts (inset). **Panel I**: (grade 4): the bone surface is very irregular with many osteoclasts (inset), with no osteoblasts visible. **Panels J–L, osteomyelitis**: (bar length 1 cm; inset bar 50 μm). **Panel J**: (grade 1): note the presence of a single inflammatory cell focus in the bone marrow (inset); the rest of the whitish-stained fatty bone marrow shows no changes. **Panel K**: (grade 3): note the large bone marrow areas filled with blue-stained, inflammatory cells (inset); in the whitish-stained areas fibrous tissue is predominant. **Panel L**: (grade 4): nearly all the bone marrow is filled with inflammatory cells and cellular debris (inset). **Panels M–O, bacterial infection**: (bar 100 μm, inset bar 10 μm [oil immersion]). **Panel M**: (grade 1): note the presence of a bacterial colony in the slightly inflamed bone marrow **(Panel M)**; bacteria have filiform and coccoid morphology (inset). **Panel N**: (grade 3): note the myriad bacteria on the denuded bone surface and a few micrometers into the bone; the higher magnification again shows a mixed bacterial population (inset). **Panel O**: (grade 4): note the very large number of bacterial colonies spreading into deeper areas of the bone stock. **Panels P–R, empyema in the canalis mandibularis**: (bar 2 mm; inset bar 20 μm). **Panel P**: (grade 2): note the presence of pus formed by cellular debris mixed with coccoid bacteria (inset) in the mandibular canal. **Panel Q**: (grade 3): note the large amount of pus in the mandibular canal (inset). **Panel R**: (grade 5): the mandibular canal is completely filled with pus; multifocal Splendor-Hoeppli granula are observed (inset). Methanol-fixed, undecalcified, MMA-embedded, Giemsa-eosin-stained mandibular tissue sections from minipigs treated with zoledronate. **Panels S–U, periosteal bone proliferation in the corpus mandibulae**: (bar 1 mm; inset bar 100 μm). **Panel S**: (grade 1): note the periosteal formation of a minimal amount of trabecular bone at the corpus. **Panel T**: (grade 3): periosteal bone formation (trabecular) reaches nearly the same thickness as the original cortex (solid). **Panel U**: (grade 4): note the marked periosteal formation of new bone, all of trabecular type, and the ongoing proliferation characterized by the large number of cuboid-shaped, active osteoblasts lining the reddish-pink bone matrix, and ovoid-shaped osteocytes entrapped in the matrix (inset).

Table 3
Microscopic grading scheme for semi-quantitative light microscopic scoring (*concomintant presence of these two hallmark parameters together defines BRONJ): grade 1 = minimal, grade 2 = slight, grade 3 = moderate, grade 4 = marked/severe, grade 5 = massive.

Histological change	Diagnostic term	Grade[1]
Inflammation of gingiva	Gingivitis	0–5
Inflammation of periodontium	Periodontis	0–5
Inflammation of tooth root cavities	Pulpitis	0–5
Presence of non-viable bone or tooth particles	Sequester formation	Not graded (P)
Inflammation of bone and bone marrow	Osteomyelitis	0–5
Inflammation in canalis mandibularis	Empyema	0–5
Presence of Giemsa-positive bacterial colonies	Bacterial infection	0–5
Presence of sulfur granules (Splendor-Hoeppli material)	Characteristic of Actinomyces spp.	0–5
Number of osteoblasts lining the trabecular surface	Bone formation	0–5
Irregular trabecular surface lining (Howship lacunae) with/without presence of osteoclasts	Osteolysis	0–5
Presence of empty osteocytic lacunae (foci of $n > 5$)	Osteonecrosis	0–5
Discontinuation of oral mucosa	Low-grade gingival erosion/ulceration	1–2
With orally exposed/denuded bone (showing bluish-staining in illumination with fluorescent light)	High-grade gingival ulceration*	3–5
Destruction of extracellular matrix* (showing bluish fluorescence of osteolytic areas)	Demineralization*	0–5
Trabecular-type new bone formation at the corpus mandibulae	Peri- or endosteal bone proliferation	0–5

receiving zoledronic acid alone showed lower mean HU values, but because of the large variation no conclusions could be made. The mean attenuation value directly under extraction site was always significantly lower in the group that developed MRONJ, in comparison with the control (tooth extraction only) animals, which received no zoledronic acid (891 ± 119 HU and 1172 ± 199 — HU mean and SD, respectively).

3.2.3. XtremeCT

A more detailed analysis of some parameters was performed using microCT scans. Bone volume (BV) and bone mineral density (BMD) were assessed in the area surrounding the PM4 extraction site, and in a larger area between PM2 and M3. An increased BV was associated with animals that had developed BRONJ. In the area surrounding the extraction site there was a significant BMD decrease in animals that had developed MRONJ. There was a good correlation ($R^2 = 0.96$) between these findings and the results for mean attenuation obtained from clinical CT. In the second area, between PM2 and M3, some of animals that had received zoledronic acid showed lower BMD values. Again, however, the variation prevented conclusions being drawn, suggesting that this is not a useful diagnostic marker.

3.3. Microscopic changes

The most obvious microscopic change observed was slight to massive inflammation of bone marrow and bone stock of the jaws around the extraction sites. The inflammation was characterized by an infiltration of mixed inflammatory cells (chronic osteomyelitis). This profound inflammation of the jaw was not only present in the medullary area, but also in form of pus accumulation in the maxillary sinus, as well as in the mandibular canal (empyema), which were exclusively found in animals treated with zoledronic acid with or without tooth extraction. Additional inflammation was recorded more superficially in the gingiva and periodontium, in the form of diffuse or focal (micro abscesses) cell infiltration, and in the pulp cavity of adjacent teeth (pulpitis) in animals of all groups. These changes were often accompanied by plant material, originating from food in the oral cavity. The deep as well as the superficial inflammations were associated with the presence of moderate to large amounts of bluish-stained Giemsa-positive bacterial colonies (infection), multifocally present in the bone marrow and mandibular canal, as well in and on the gingival epithelium and at the bone surface. Furthermore, the mandibulary empyema sometimes included deposition of sulfur granules (Splendor-Hoeppli material), which is morphologically characteristic of infection by Actinomyces spp. In this context, it is important to mention that superficial gingivitis, along with bacteria, was also recorded in control animals (not treated with zoledronic acid). However, the slight to massive inflammation of the bone marrow and mandibular canal was only recorded in the two groups treated with zoledronic acid, even in the absence of concurrent iatrogenic tooth extraction.

Markedly reduced bone formation was recorded microscopically in the bone stock, featuring very low numbers of osteoblasts lining the bone trabeculi. Alongside this, a marked increase in bone resorption was recorded, characterized by an irregular trabecular surface lining, showing deep indentations (Howship lacunae). Both changes were more pronounced in animals treated with zoledronic acid, and led to a marked reduction in bone density, readily visible through macroscopic observation of the stained slides and to the naked eye on contact radiographs. Most of the lacunae were empty, however, large, multifocal, multinuclear osteoclasts were seen at these degradation zones. This indicated ongoing active bone degradation by osteoclasts. Another characteristic change at the bone stock was the multifocal, patchy-to-diffuse presence of empty osteocytic lacunae — the microscopic hallmark of osteonecrosis. However, the mineralized extracellular matrix of these trabeculi showed no obvious signs of degradation. In contrast, minimal-to moderate-grade demineralization of bone matrix was recorded at the bone surface of the empty tooth extraction sites exclusively in all animals treated with zoledronic acid and that had undergone tooth extraction. In these cases, the denuded bone exposed to the oral cavity showed brownish discoloration and destruction of the mineralized bone matrix. In contrast, animals only treated with zoledronic acid, showed complete epithelial coverage and absence of bone demineralization.

4. Discussion

This study assessed multiple macroscopic, radiological, and histological parameters in animals that did or did not develop MRONJ-associated changes after bisphosphonate administration. From each of the three study groups, a few easy-to-perform and clinically relevant parameters were chosen (Table 4) to devise a scoring system. This scoring system can be used to design and monitor studies aimed at therapy and prevention models. Results of the studies can be compared with already existing databases and templates. The system provides information about a set of established methods and can make studies more effective and comparable with each other.

Table 4
Clinically relevant parameters chosen to devise the scoring system.

Clinical		Radiological		Histological	
Exposed necrotic bone	1–10	Healing of extraction socket	Presence/absence	High-grade gingival ulceration with orally exposed bone	3–5
Fistula/abscess	0–5	Peri/endosteal reaction	0–5	Demineralization of extracellular matrix of denuded bone areas	0–5
Purulent discharge	1–3	Soft tissue swelling	0–5	Osteonecrosis (foci of $n > 5$ empty lacunae)	0–5
Soft tissue swelling	1–3	Apparent density of trabecular bone under extraction site	HU value	Bacterial osteomyelitis	0–5
Gingivitis	1–3	Empyema	Presence/absence	Empyema	0–5

MRONJ is associated with high morbidity and adversely affects patients' quality of life. Authors of a position paper from 2014 urged researchers to perform research using animal models to validate or establish new treatment or prevention strategies (Ruggiero et al., 2014). The minipig is a well-established MRONJ animal model, with advantages over dog, sheep, or rodent models (Pautke et al., 2012; Otto et al., 2017). The scoring system described in Table 3 can be used in future studies of MRONJ in minipig models, to produce more tangible results. Parameters chosen for this system are relatively simple to assess, and can provide an indication of the severity of the pathological changes associated with MRONJ.

4.1. Macroscopic parameters

Exposed necrotic bone is a hallmark of macroscopic presentation of MRONJ. Fistula and abscess formation are often associated changes (Phal et al., 2007). Purulent discharge is a sign of infection associated with later stages of MRONJ. Soft tissue swelling and gingivitis are non-specific, subtle changes associated with inflammation.

4.2. Clinical parameters

MRONJ is defined as exposed necrotic bone, so this is an obvious parameter. Fistula that penetrates the jaw was added to MRONJ definition in a 2014 position paper (Ruggiero et al., 2014). Purulent discharge is associated with the above two factors, and is evidence of an infection. Soft tissue swelling and gingivitis are non-specific and non-dramatic parameters, but they should draw attention and changes should be noted.

Common radiological signs of human MRONJ include persisting alveolar sockets after tooth extractions, due to a lack of remodeling, and a mixed pattern of radiolucent and radiopaque areas. Radiolucent areas can occur in the centre of MRONJ lesions, where bone has already been severely degraded. Areas surrounding the necrotic bone lesions are often characterized by bone sclerosis, which might be due to the reaction of viable bone. These areas can be large and might even dominate the radiological representation of MRONJ (citation 17 and 19).

In our model, persisting alveolar sockets and lower HU values were found in the area directly beneath the tooth extraction, coinciding exactly with the main MRONJ area identified histologically. This is in line with the well-known effects of remodeling suppression under antiresorptive drugs and bone degradation in MRONJ lesions, which was also observed in our histological analysis. However, we did not find the pronounced sclerosis in surrounding bone observed in humans, even though periosteal swelling and bone proliferation were already present on the base of the mandible. The possible explanation of this issue could be that MRONJ in humans is a slowly developing process, with sclerosis developing as a consequence of chronic inflammation. In the animal model, the induction time is more acute because it is not feasible to wait years to develop long-term chronic inflammatory foci or chronic osteomyelitis. This results in a difference in how MRONJ develops. Nevertheless, changes in HU values were our most significant finding and should be used both for human and animal studies.

The decrease in cortical bone density was similar in scans performed with clinical CT and microCT. Since it is possible to perform clinical CT on patients, and there is a good correlation between BMD and radio intensity (Schreiber et al., 2011), only clinical CT was included in the scoring, with microCT results used as a control for our findings. The method used was adopted from another publication (Hamada et al., 2014) and modified to fit more to the minipig model. Empyema formation is a manifestation of infection and is associated with more severe stages of MRONJ in humans (stages 2 and 3) (Ruggiero et al., 2014). It is therefore important to identify the severity of the disease.

n this study the MRONJ model was created using intravenous injections of BPs and tooth extraction, as described by Pautke. In both BP-treated groups MRONJ-associated changes were similar. In the group that did not undergo tooth extraction it was not possible to assess healing of the extraction socket, but cases of spontaneous MRONJ were observed and were associated with issues such as food impaction, which were likely to damage the mucosal surface. With the help of these results, future MRONJ studies in minipigs aimed at therapy and prevention could have more tangible and consistent results.

There are some limitations of this study. There are numerous parameters that could be used in a scoring system. Those used in this study were selected by the authors, so perhaps there are some parameters that could better serve this purpose. The chosen parameters were selected because they had to be relatively easy to perform and to show a clear difference between animals that did develop MRONJ and those that did not.

The whole study was carried out using Göttingen minipigs, so the authors can only hypothesize that this scoring system is appropriate for other animal models of MRONJ. It is possible, but further studies are warranted to support this hypothesis. Nevertheless, the scoring system can provide a basis for more consistent characterization of future MRONJ studies. Studies that can replicate these results and similar studies on different species are recommended to increase the scientific basis of these findings.

Histological analysis of MRONJ-related changes helped to better characterize this relatively new, preclinical, large model for MRONJ. Preliminary histological evaluation of large animal models has been performed before in dogs (Allen et al., 2010, 2011; Huja et al., 2011), and in minipigs (Pautke et al., 2012). However, these groups used decalcified, paraffin-embedded, and hematoxylin-eosin-stained tissue slides. With changes in the bone tissue predominating in MRONJ, a cutting-grinding technique, using non-decalcified, MMA-embedded material stained with Giemsa-eosin — a special stain often used in bone histology — may be more effective in highlighting histological changes compared with the use of standard HE-staining of paraffin-embedded material.

The most obvious histopathological change found in this animal model was active osteomyelitis, along with bacterial infection, a

finding also characteristic for MRONJ in human patients (Lesclous et al., 2009; Ji et al., 2012). Infections with Actinomyces spp. are often identified using bacteriological analysis of biopsy samples (Chiandussi et al., 2006). This feature was also found in this animal model, where sulfur granules in the maxillary and mandibular empyema were described, this morphologically characterizing the involvement of Actinomyces spp. Currently, it is unclear whether these bacteria are a causal pathogen or only an accompanying feature of otherwise affected bone stock. In this context, it is important to note that these non-obligatory-pathogenic bacteria are commonly found in the oral fauna of pigs (and humans), can enter the bone tissue via open wounds (e.g. after surgical tooth extraction) or via ubiquitous, small, epithelial changes in the gingiva, and may therefore represent only concomitant infections. Both incomplete gingival coverage of the tooth extraction sites as well as multifocal gingivitis and periodontitis (Kos, 2014), along with microscopic evidence of food material (all found in this model), facilitate such bacterial inoculation.

The low numbers of osteoblasts lining the bone trabeculi represented a marked affection of bone formation; this was only recorded in ZOL-treated animals (groups 1 and 2). It is important to note that this finding was not only recorded at the tooth extraction sites, but also in the contralateral areas without tooth extraction, which may give important clues regarding the principal pathological importance of BP treatment in inducing MRONJ. Along with the pronounced osteoclastic bone resorption — more pronounced in animals in groups 1 and 2 — BP treatment caused a marked reduction in bone density. Furthermore, the presence of empty osteocytic lacunae — the characteristic microscopic feature of osteonecrosis — was more pronounced at the extraction sites in ZOL-treated animals (group 1 and 2). On the contralateral sides without tooth extraction the severity was comparable with the non-ZOL-treated animals of group 3, where low-grade osteonecrosis could also be observed. Finally, osteolysis of low to moderate severity, along with exposure of denuded bone to the oral cavity, was exclusively found in animals of group 2. By applying fluorescence illumination to histological sections, the osteolytic areas could be easily identified due to the prior exposure of the animal to doxycycline. This feature can also be used in clinical characterization and therapy when combined with tetracycline, a commonly used antibiotic (Pautke et al., 2010, 2011).

The osteolysis was consistent in the lower jaw (all six mandibular extraction sites were affected). The ZOL-treated animals of group 1 — without tooth extraction — did not show this change. Therefore, the destruction of extracellular matrix at the denuded bone surface is the sole microscopic hallmark of MRONJ-like changes in this animal model. This raises the important issue of BP treatment in the presence of large, iatrogenic wounds. Animals in group 3, which were not treated with BP but had large open wounds after tooth extraction, only had low-grade inflammation of the gingiva, and showed no deeper indications, such as osteomyelitis, empyema, or osteolysis of exposed bone.

5. Conclusion

This study proposes and describes clinical, radiological, and histological parameters that can be used for scoring of MRONJ in a minipig model. The clinical parameters include exposed, necrotic bone, fistula formation, and inflammation. Radiological parameters include lack of extraction socket healing, decrease in attenuation in bone beneath the extraction site, and periosteal reaction. Histological parameters include osteolysis of extracellular bone matrix and bone denudation. These parameters make up a valid tool for designing and assessing MRONJ therapy and prevention studies in minipig models. The system could be used in other large animal models, such as sheep (Voss et al., 2016), but this would require further validation. The radiological parameters indicated may also be of value in the clinical diagnosis and staging of MRONJ patients.

Further investigation of changes in animal models may help to answer open questions regarding the pathogenesis of MRONJ, as well as its prevention or treatment.

Conflicts of interest

This work was supported by an AOCMF R&D Commission AO Foundation grant.

References

Allen MR, Kubek DJ, Burr DB: Cancer treatment dosing regimens of zoledronic acid result in near-complete suppression of mandible intracortical bone remodeling in beagle dogs. J Bone Miner Res 25(1): 98–105, 2010

Allen MR, Kubek DJ, Burr DB, Ruggiero SL, Chu TM: Compromised osseous healing of dental extraction sites in zoledronic acid-treated dogs. Osteoporos Int 22(2): 693–702, 2011

Arce K, Assael LA, Weissman JL, Markiewicz MR: Imaging findings in bisphosphonate-related osteonecrosis of jaws. J Oral Maxillofac Surg 67(Suppl. 5): 75–84, 2009

Cheung A, Seeman E: Teriparatide therapy for alendronate-associated osteonecrosis of the jaw. N Engl J Med 363(25): 2473–2474, 2010

Chiandussi S, Biasotto M, Dore F, Cavalli F, Cova MA, Di Lenarda R: Clinical and diagnostic imaging of bisphosphonate-associated osteonecrosis of the jaws. Dentomaxillofac Radiol 35(4): 236–243, 2006

Hamada H, Matsuo A, Koizumi T, Satomi T, Chikazu D: A simple evaluation method for early detection of bisphosphonate-related osteonecrosis of the mandible using computed tomography. J Craniomaxillofac Surg 42(6): 924–929, 2014

Hatoum HT, Lin SJ, Smith MR, Barghout V, Lipton A: Zoledronic acid and skeletal complications in patients with solid tumors and bone metastases: analysis of a national medical claims database. Cancer 113(6): 1438–1445, 2008

Huja SS, Mason A, Fenell CE, Mo X, Hueni S, D'Atri AM, et al: Effects of short-term zoledronic acid treatment on bone remodeling and healing at surgical sites in the maxilla and mandible of aged dogs. J Oral Maxillofac Surg 69(2): 418–427, 2011

Hutchinson M, O'Ryan F, Chavez V, Lathon PV, Sanchez G, Hatcher DC, et al: Radiographic findings in bisphosphonate-treated patients with stage 0 disease in the absence of bone exposure. J Oral Maxillofac Surg 68(9): 2232–2240, 2010

Ji X, Pushalkar S, Li Y, Glickman R, Fleisher K, Saxena D: Antibiotic effects on bacterial profile in osteonecrosis of the jaw. Oral Dis 18(1): 85–95, 2012

Khosla S, Burr D, Cauley J, Dempster DW, Ebeling PR, Felsenberg D, et al: Bisphosphonate-associated osteonecrosis of the jaw: report of a task force of the American society for bone and mineral research. J Bone Miner Res 22(10): 1479–1491, 2007

Kos M: Association of dental and periodontal status with bisphosphonate-related osteonecrosis of the jaws. A retrospective case controlled study. Arch Med Sci 10(1): 117–123, 2014

Kumar V, Sinha RK: Evolution and etiopathogenesis of bisphosphonates induced osteonecrosis of the jaw. N Am J Med Sci 5(4): 260–265, 2013

Lesclous P, Abi Najm S, Carrel JP, Baroukh B, Lombardi T, Willi JP, et al: Bisphosphonate-associated osteonecrosis of the jaw: a key role of inflammation? Bone 45(5): 843–852, 2009

Major P, Lortholary A, Hon J, Abdi E, Mills G, Menssen HD, et al: Zoledronic acid is superior to pamidronate in the treatment of hypercalcemia of malignancy: a pooled analysis of two randomized, controlled clinical trials. J Clin Oncol 19(2): 558–567, 2001

Marx RE: Pamidronate (Aredia) and zoledronate (Zometa) induced avascular necrosis of the jaws: a growing epidemic. J Oral Maxillofac Surg 61(9): 1115–1117, 2003

Migliorati CA: Bisphosphanates and oral cavity avascular bone necrosis. J Clin Oncol 21(22): 4253–4254, 2003

Novince CM, Ward BB, McCauley LK: Osteonecrosis of the jaw: an update and review of recommendations. Cells Tissues Organs 189(1–4): 275–283, 2009

Otto S, Pautke C, Martin Jurado O, Nehrbass D, Stoddart MJ, Ehrenfeld M, et al: Further development of the MRONJ minipig large animal model. J Craniomaxillofac Surg 45(9): 1503–1514, 2017

Pautke C, Bauer F, Bissinger O, Tischer T, Kreutzer K, Steiner T, et al: Tetracycline bone fluorescence: a valuable marker for osteonecrosis characterization and therapy. J Oral Maxillofac Surg 68(1): 125–129, 2010

Pautke C, Bauer F, Otto S, Tischer T, Steiner T, Weitz J, et al: Fluorescence-guided bone resection in bisphosphonate-related osteonecrosis of the jaws: first clinical results of a prospective pilot study. J Oral Maxillofac Surg 69(1): 84–91, 2011

Pautke C, Kreutzer K, Weitz J, Knodler M, Munzel D, Wexel G, et al: Bisphosphonate related osteonecrosis of the jaw: a minipig large animal model. Bone 51(3): 592–599, 2012

Phal PM, Myall RW, Assael LA, Weissman JL: Imaging findings of bisphosphonate-associated osteonecrosis of the jaws. AJNR Am J Neuroradiol 28(6): 1139–1145, 2007

Ruggiero SL, Dodson TB, Assael LA, Landesberg R, Marx RE, Mehrotra B, et al: American Association of Oral and Maxillofacial Surgeons position paper on bisphosphonate-related osteonecrosis of the jaws — 2009 update. J Oral Maxillofac Surg 67(Suppl. 5): 2–12, 2009

Ruggiero SL, Dodson TB, Fantasia J, Goodday R, Aghaloo T, Mehrotra B, et al: American Association of Oral and Maxillofacial Surgeons position paper on medication-related osteonecrosis of the jaw — 2014 update. J Oral Maxillofac Surg 72(10): 1938–1956, 2014

Sambrook P, Cooper C: Osteoporosis. Lancet 367(9527): 2010–2018, 2006

Schreiber JJ, Anderson PA, Rosas HG, Buchholz AL, Au AG: Hounsfield units for assessing bone mineral density and strength: a tool for osteoporosis management. J Bone Jt Surg Am 93(11): 1057–1063, 2011

Torres SR, Chen CS, Leroux BG, Lee PP, Hollender LG, Santos EC, et al: Mandibular cortical bone evaluation on cone beam computed tomography images of patients with bisphosphonate-related osteonecrosis of the jaw. Oral Surg Oral Med Oral Pathol Oral Radiol 113(5): 695–703, 2012

Voss PJ, Stoddart MJ, Bernstein A, Schmelzeisen R, Nelson K, Stadelmann V, et al: Zoledronate induces bisphosphonate-related osteonecrosis of the jaw in osteopenic sheep. Clin Oral Investig 20(1): 31–38, 2016

Wang J, Goodger NM, Pogrel MA: Osteonecrosis of the jaws associated with cancer chemotherapy. J Oral Maxillofac Surg 61(9): 1104–1107, 2003